MAGNETIC FIELD CONFIGURATIONS ASSOCIATED WITH POLARITY INTRUSION IN A SOLAR ACTIVE REGION

I. *The Force-Free Fields*

B. C. LOW

High Altitude Observatory, National Center for Atmospheric Research, Boulder, Colo., U.S.A.*

(Received 12 May, 1981)

Abstract. This paper presents a new class of exact solutions describing the non-linear force-free field above a spatially localized photospheric bipolar magnetic region. An essential feature is the variation in all three Cartesian directions and this could not be modelled adequately with previously known symmetric force-free fields. Sequences of force-free fields are constructed and analyzed to simulate the slow growth of a pair of spots on the photosphere. The axis connecting the spots executes rotational motion, distorting the photospheric neutral line separating fluxes of opposite signs. We show directly from the analytic solutions that the resulting reversal of the positions of the spots relative to the background field is associated with (i) the creation of magnetic free energy, (ii) the severe shearing of localized low-lying loops in the vicinity where the photospheric transverse field aligns with the photospheric neutral line, and (iii) the emergence and disappearance of flux from the photosphere at these highly stressed regions. The model relates theoretically for the first time these different magnetic field features that have been suggested by observation and theoretical considerations to be flare precursors. A general formula, based on the virial theorem, is also given for the free energy of a force-free field, strictly in terms of the field value at the photosphere. This formula has obvious practical application.

1. Introduction

The evolution of solar magnetic fields through successive force-free states has been studied with mathematical models by many people (Low, 1981a, and references therein). These models were aimed at describing the quasi-steady magnetic fields in the solar active region. The force-free assumption seems reasonable since the active region field is typically a few hundred gauss or more and the plasma beta is much smaller than unity (Gold, 1964). With these models, a full MHD description of the field evolution is avoided and as a first approximation, we need to solve a sequence of static-elliptic problems.

The magnetic field evolves as the result of photospheric motions and the transport of magnetic flux through the photosphere. Much of the modelling effort so far has concentrated on the effect of only the photospheric motions of the magnetic footpoints, with the interest of knowing how a magnetic field evolves to a critical configuration for a flare or other eruptions to occur (Low, 1977a, b, 1980a; Jockers, 1978; Birn *et al.*, 1978; Priest and Milne, 1980; Su, 1980). The basic effect is nonlinear and to render the problem tractable, it has been popular to treat the two dimensional Cartesian system. The independence of the third Cartesian coordinate

* The National Center for Atmospheric Research is sponsored by the National Science Foundation.

Solar Physics **77** (1982) 43–61. 0038–0938/82/0771–0043 $02.85.

gives rise to an arcade-like geometry. This model proved useful for the theoretical demonstration of basic properties, but it does not give insight into realistic situations with three dimensional variation. The interest of this paper is in the situation of a bipolar pair of spots having formed in the photosphere amidst a background field. As the spots grow in size and execute proper motion, electric currents are generated in the electrically highly conducting atmosphere. This manifests in the twisting of the 'frozen-in' field lines. Such a setting is widely accepted to be prone to flare eruptions (Zirin, 1974). Of particular interest is the case where the pair of spots rotates around to reverse the positions of the leading and following polarities, causing each spot to intrude into a region of opposite polarity (see, e.g., Zirin, 1970a, b; Zirin and Tanaka, 1973; Zirin and Lazareff, 1975; Rust, 1976). A two-dimensional consideration will clearly not be adequate.

The study of solar magnetic fields is limited by two difficulties. The first is that only the photospheric magnetic field can be measured to fine spatial resolutions (Beckers, 1971; Harvey, 1977; Stenflo, 1978). It is therefore necessary to extrapolate theoretically for the field above the photosphere from their measured photospheric values. The second difficulty is that, even within the force-free approximation which conveniently decouples the influence of the plasma, this extrapolation is an intractable nonlinear problem (Schmidt, 1968; Sakurai, 1981a). In consequence, our knowledge of the magnetic field structures above the photosphere must rely on a synthesized picture based on magnetograms, Hα morphology of chromospheric fibrils, X-ray pictures of plasma loops and so on (see, e.g., Švestka, 1976; Sturrock, 1980). It will be useful to find exact solutions of force-free fields through which the various field structures, implied by different sets of observational data, can be related in a unified manner.

The equations for a force-free field $\mathbf{B}$ are:

$$\nabla \times \mathbf{B} = \alpha \mathbf{B}\,, \tag{1}$$

$$(\mathbf{B} \cdot \nabla)\alpha = 0\,, \tag{2}$$

where α is a scalar function. The problem for a constant α is a completely solvable linear problem (Chandrasekhar and Kendall, 1957; Nakagawa and Raadu, 1972) but there is no physical justification for assuming α to be constant everywhere. It is, in fact, easy to show that the nonlinear non-constant α fields are the ones more likely to be found in nature (Sakurai, 1979; Low, 1981a). As for these nonlinear fields, known solutions are restricted to highly symmetric ones such as the above two dimensional Cartesian system or the cylindrically symmetric system (Lüst and Schlüter, 1954; Barnes and Sturrock, 1972). For the purpose of this paper, another class of nonlinear force-free fields will be considered. These fields possess a high degree of mathematical symmetry if transformed into a suitable coordinate system with the advantage that the force-free equations (1) and (2) can be solved trivially in closed form. However, their symmetry imposes no serious restriction on the geometry of the situation we are interested in, namely, that of an isolated bipolar magnetic region.

2. Model Construction

Consider an initial potential field $\mathbf{B}_{\text{pot}}$ in the half space bounded below by the plane $z = 0$ representing the photosphere:

$$\mathbf{B}_{\text{pot}} = B_0\left(0, \frac{-a(z+a)}{y^2+(z+a)^2}, \frac{ay}{y^2+(z+a)^2}\right), \tag{3}$$

where B_0 and a are constants. We use Cartesian coordinates x, y, and z. The potential field is produced by an infinite straight line current running along the line $y = 0$, $z = -a$ below the photosphere. Suppose the magnetic field evolves as the result of photospheric motion and the transport of flux through the photosphere. If we assume the process to be very slow and at each instant of time, the field is force-free, we would then need to solve Equations (1) and (2) subject to the distribution of the photospheric normal flux,

$$B_z(x, y, 0) = B_n(x, y), \tag{4}$$

where $B_n(x, y)$ is given at each instant of time. Let us take the electrical conductivity to be infinite and regard the plasma to be frozen into the magnetic field. The above boundary value problem is complicated by the need to account for the evolutionary history, relating footpoints, one to another, in terms of field line connectivity (Sturrock and Woodbury, 1967). A different field line connectivity for the same boundary condition (4) can give a different force-free field. This is evidently an intractable problem. Our need in this paper to allow for variation in all x, y, and z coordinates is an added burden.

Let us now impose some purely mathematical symmetry to the above problem to make the problem tractable without compromising on the essential physical feature of varying in all three Cartesian directions. Set up a spherical polar coordinate system with its origin located at $(0, 0, -a)$ in the Cartesian system, and with the polar axis located on the line $y = 0$, $z = -a$ along which lies the line current responsible for the potential field $\mathbf{B}_{\text{pot}}$. The relationship between the two coordinate systems is sketched in Figure 1. The next step is to make the ansatz that the force-free field in the above situation of flux emergence is axially symmetric in the polar coordinate system. This means that the magnetic field is of the form

$$\mathbf{B} = \frac{1}{r \sin \vartheta}\left[\frac{1}{r}\frac{\partial U}{\partial \vartheta}\mathbf{r} - \frac{\partial U}{\partial r}\boldsymbol{\vartheta} + V(U)\boldsymbol{\phi}\right] \tag{5}$$

in the usual polar notation, where V is a free function of one variable and the force-free equations (1) and (2) reduce to the scalar equation:

$$\frac{\partial^2 U}{\partial r^2} + \frac{\sin \vartheta}{r^2}\frac{\partial}{\partial \vartheta}\left(\frac{1}{\sin \vartheta}\frac{\partial U}{\partial \vartheta}\right) + V(U)\frac{\mathrm{d}V(U)}{\mathrm{d}U} = 0, \tag{6}$$

with

$$\alpha = \frac{\mathrm{d}V(U)}{\mathrm{d}U}. \tag{7}$$

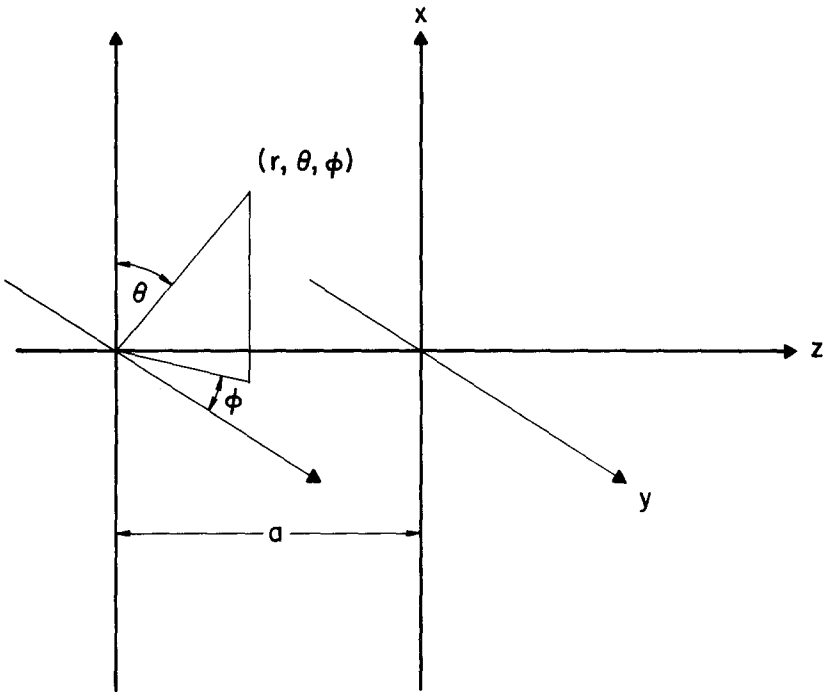

Fig. 1. Positioning of the polar coordinate system.

These axisymmetric fields were considered previously by Morikawa (1969), Cohen *et al.* (1973), and Milsom and Wright (1976). It follows that we can generate sequences of models for an isolated biopolar region by taking force-free field solutions of this axisymmetric system and transforming them to the Cartesian coordinate system in Figure 1. In this way, we obtain specific models without having to solve directly the above boundary value problem with the complicated condition of field line connectivity. In effect, we have turned the mathematical problem around, by giving the force-free field directly and using it to determine the field line connectivity and the boundary condition (4). The usefulness of such an approach becomes clear from the physically interesting models that we now proceed to construct.

Equation (6) is nonlinear and a numerical treatment is in general necessary. There is a special case for which its complete integral can be written down in close form, namely, when U is a strict function of r and Equation (6) integrates to give

$$\left(\frac{\mathrm{d}U}{\mathrm{d}r}\right)^2 + [V(U)]^2 = A^2, \tag{8}$$

where A is a constant. It follows from Equations (5) and (7) that, with $A = B_0 a$,

$$\mathbf{B} = \frac{B_0 a}{r \sin \vartheta} [\cos \varphi(r) \boldsymbol{\vartheta} + \sin \varphi(r) \boldsymbol{\phi}] \tag{9}$$

and

$$\alpha = \frac{\mathrm{d}\varphi(r)}{\mathrm{d}r}, \tag{10}$$

where φ is a free generating function. Equation (9) describes a vector of magnitude $B_0 a/r \sin\vartheta$ lying in the spherical surface of radius r. The generating function $\varphi(r)$ is the orientation of this vector for a given spherical surface. As we move through successive spherical surfaces of increasing r, the vector orientation would vary according to $\varphi(r)$. A simple transformation from the spherical to the Cartesian coordinate systems gives the magnetic field components:

$$B_x = -\frac{B_0 a}{r}\cos\varphi(r), \tag{11}$$

$$B_y = \frac{B_0 axy}{r[y^2+(z+a)^2]}\cos\varphi(r) - \frac{B_0 a(z+a)}{y^2+(z+a)^2}\sin\varphi(r), \tag{12}$$

$$B_z = \frac{B_0 ax(z+a)}{r[y^2+(z+a)^2]}\cos\varphi(r) + \frac{B_0 ay}{y^2+(z+a)^2}\sin\varphi(r), \tag{13}$$

where $r^2 = x^2+y^2+(z+a)^2$. At the photosphere $z=0$, the normal field distribution is

$$B_n(x,y) = B_z(x,y,0) = \frac{B_0 a^2 x}{(x^2+y^2+a^2)^{1/2}(y^2+a^2)}\cos\varphi[(x^2+y^2+a^2)^{1/2}] + \\ + \frac{B_0 ay}{y^2+a^2}\sin\varphi[(x^2+y^2+a^2)^{1/2}]. \tag{14}$$

In the following section, we discuss the morphology of these force-free fields as generated by specific sequences of the generating function φ.

3. Magnetic Field Morphology

The first thing to notice is that setting $\varphi = \pi/2$ for all r gets us the initial potential field $\mathbf{B}_{\mathrm{pot}}$. This is clear from Equation (9) which gives, for $\varphi = \pi/2$, the potential field due to a line current running along the polar axis.

Next consider the generating function

$$\varphi = \varphi_0 + (\varphi_1 - \varphi_0)(r-a)/(r_0-a), \qquad r \leqq r_0$$
$$= \varphi_1, \qquad r > r_0, \tag{15}$$

where φ_0, φ_1, and r_0 are constants. Thus, φ increases from φ_0 to φ_1 linearly with r until $r = r_0$, beyond which φ is constant at φ_1. The associated magnetic field is force-free with a constant α (see Equation (10)) in the space $r \leqq r_0$ whereas outside $r \leqq r_0$, the field is just the undisturbed potential $\mathbf{B}_0$. In physical terms, we are looking at field changes that are spatially located around the origin $x = y = z = 0$. Thus, α

is not constant everywhere. The magnetic field is continuous everywhere in $z > 0$ but the electric current density $\mathbf{J} = \alpha \mathbf{B}$ is discontinuous at the surface $r = r_0$ where α changes abruptly from a constant value to zero. In the perspective of the polar coordinate system, Equations (9) and (15) describe a vector whose orientation on the spherical surface $r = a$ is φ_0. As we pass through successive spherical surfaces of increasing r, the vector orientation φ increases linearly with r until $\varphi = \varphi_1$ at $r = r_0$, beyond which φ remains constant at φ_1. A smoother variation in α could have been prescribed, for example,

$$\varphi(r) = \frac{\pi}{2} \tanh\left(\frac{r}{r_0}\right), \tag{16}$$

but the properties we wish to illustrate can be appreciated just as well with the mathematically less complicated case of Equation (15).

In Figure 2, we plot the contours of constant photospheric field $B_z(x, y, 0)$ for each of these generating functions, setting $a = 1$, $r_0 = 3$. In each plot, the solid lines denote upward fluxes and the broken lines downward fluxes. Contours are spaced at intervals of $0.05 B_0$. Figure 2a shows the case of the potential field $\mathbf{B}_{\text{pot}}$ which is invariant in the x direction. Inspection of Equation (3) shows that $|B_z(x, y, 0)|$ is maximum at the location indicated. Notice that the neutral line, defined by the vanishing of $B_z(x, y, 0)$, is just the dotted straight line $y = 0$. In Figure 2b, the contours show a bipolar region resembling a pair of spots whose presence distorts the otherwise straight neutral line. For φ with increasingly steep gradients, that is, for larger values of a, these features are enhanced as shown in Figures 2c and 2d. If these contour plots were time sequence data from an active region, taken with a longitudinal field magnetograph, we would interpret them as follows. A pair of spots with opposite polarities has emerged across the neutral line of the background field. As the spots grow, they execute clockwise rotational motion. The neutral line is progressively distorted with the tendency to reverse the positions of the leading and following spots relative to the background field. One outstanding feature is the intrusion of each spot into a region of opposite magnetic polarity. The strong association of such a development with flare eruptions is well supported by specific case histories (Zirin, 1970a, b, 1972b; Zirin and Tanaka, 1973; Zirin and Lazareff, 1975; Rust, 1976; Tanaka, 1976). Let us look at this development in terms of our theoretical solution.

In a two dimensional consideration, such as the case of invariance in the x direction, distinction can be made between flux changes due to proper motion of magnetic footpoints and that due to flux emergence. With three dimensional variation, the matter is not simple. It is often quite ambiguous, looking at magnetograms, whether a spot grows because of new flux emerging locally or because there is net inward transport of pre-existing flux from nearby regions which are also evolving themselves. Zirin (1970b) cautioned that the apparent rotation of a spot may be the occurrence of new spots in successive rotated positions. In the sequence of theoretical magnetograms in Figure 2, the spots are growing in the

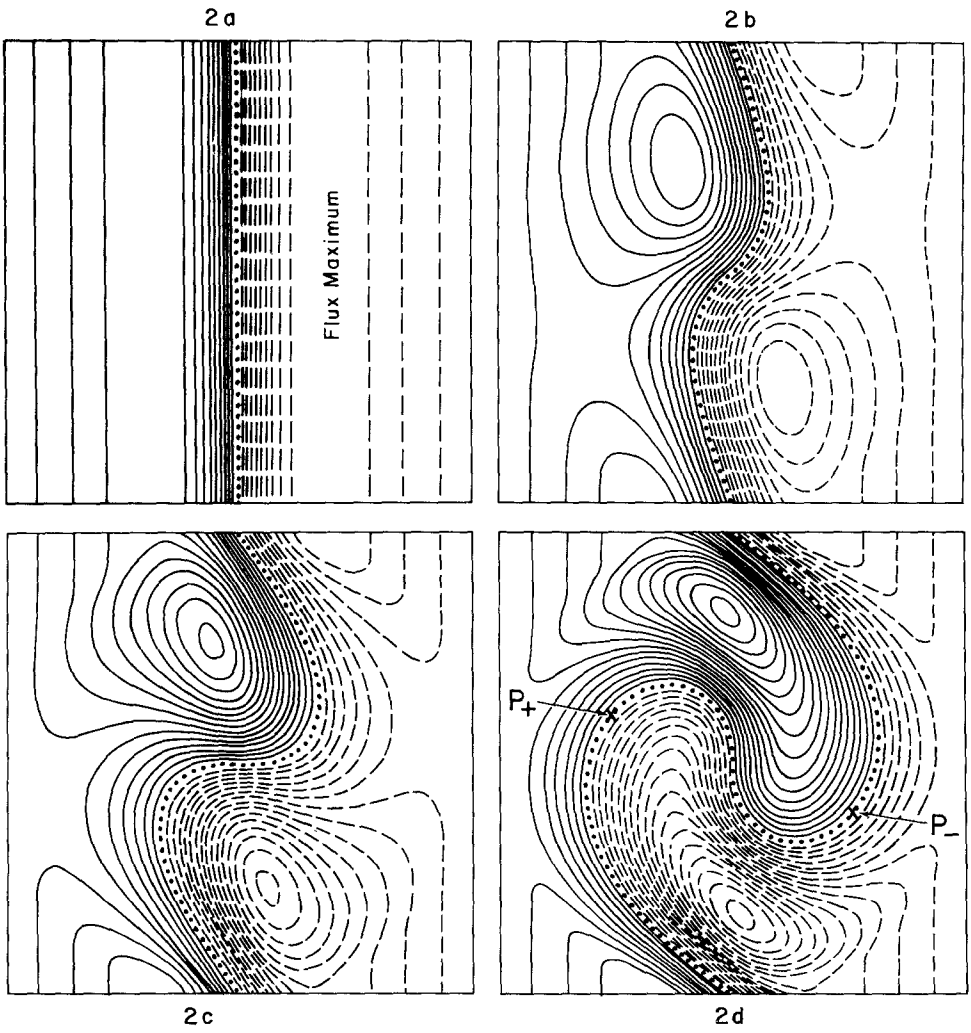

Fig. 2. Longitudinal field magnetograms for the force-free fields with $\varphi_1 = \pi/2$ and $\varphi_0 = \pi/2,\ \pi/4,\ 0, -(\pi/2)$.

sense that their forms become more pronounced and their peak field strengths increase as time progresses. The maximum values of $|B_z(x, y, 0)|$ in Figures 2a, b, c, d, are respectively 0.5, 0.65, 0.77, and 1.0, in units of B_0. However, the total flux of a given sign for the entire region decreases slightly with time. If we integrate $B_z(x, y, 0)$ of a given sign up to a circle of radius $\rho_0 = (r_0^2 - a_2)^{1/2}$ centered at the origin $x = y = 0$, the total flux of a given sign in the region $x^2 + y^2 \leqq \rho_0^2$ is

$$F = B_0 \int_0^{\rho_0} \mathrm{d}\rho 2\left(\psi \sin \psi + \frac{1}{(a^2+\rho^2)^{1/2}} \vartheta \sinh \vartheta\right), \tag{17}$$

where ψ and ϑ are given by

$$\sin\psi = (a^2+\rho^2)^{-1/2}\,\rho\cos\varphi(\sqrt{a^2+\rho^2})\,, \tag{18}$$

$$\sinh\vartheta = a^{-1}\rho\sin\varphi(\sqrt{a^2+\rho^2})\,. \tag{19}$$

We remind the reader that we have constructed $\varphi(r)$ such that field changes are confined to a finite region of space, namely $r \leqq r_0$. Figure 3a displays the integrand in Equation (17), which we denote by $f(\rho)$, for the four force-free fields. The total flux F is just the area under the curve $f(\rho)$ from $\rho = 0$ to $\rho = \rho_0$ in each case. In the sequence $\varphi_0 = \pi/2,\ \pi/4,\ 0,\ -(\pi/2)$, the total flux F decreases moderately. Hence, the growth of the pair of spots and their intrusion into regions of opposite

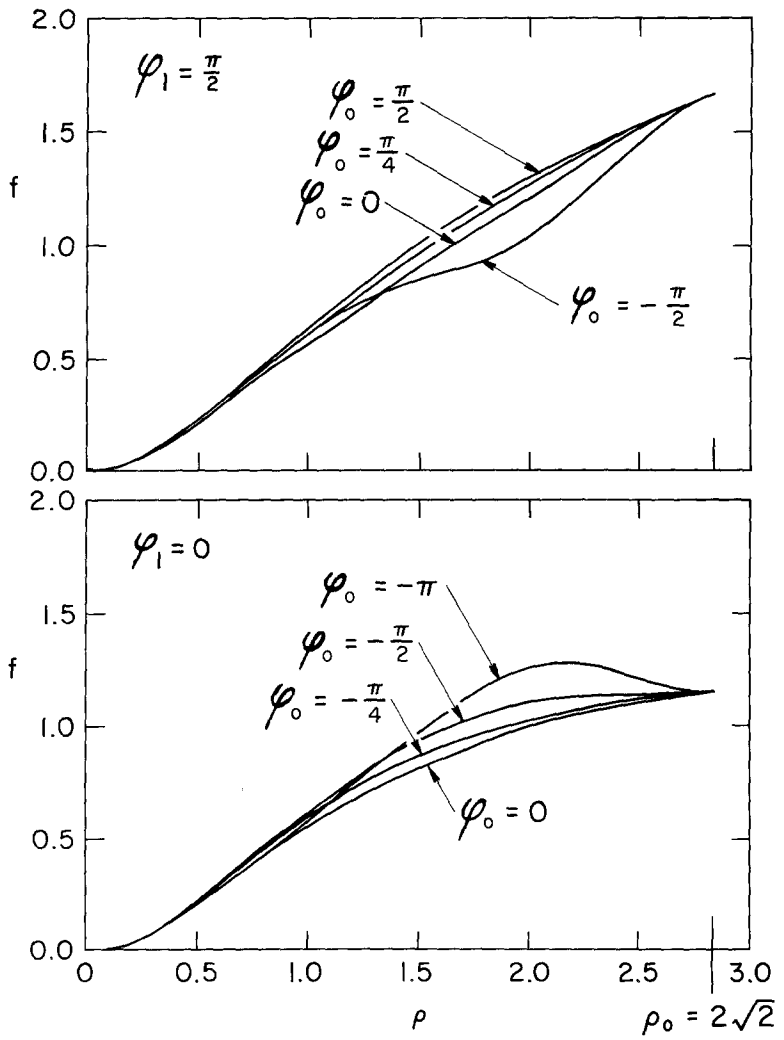

Fig. 3. The function $f(\rho)$ for (i) the force-free fields with $\varphi_1 = \pi/2$ and $\varphi_0 = \pi/2,\ \pi/4,\ 0, -(\pi/2)$, (ii) the force-free fields with $\varphi_1 = 0$ and $\varphi_0 = 0, -(\pi/4),\ -(\pi/2), -\pi$.

polarities take place with a net loss of flux below the photosphere. Another example, shown in Figure 3b, will be presented later, in which the spot motion is accompanied with a moderate increase in the total flux of one sign. The development of flaring conditions does not depend on whether the total flux is increasing or decreasing. Although flares are associated with the growth of active regions, flares at the decay phase of a sunspot are not uncommon (Zirin, 1970b). Flares must depend on the availability of free energy and the development of conditions for liberating it. This point is illustrated well by our theoretical solution. From Equation (9), the magnetic energy density is

$$|\mathbf{B}|^2/8\pi = B_0^2/8\pi \frac{a^2}{y^2+(z+a)^2} \tag{20}$$

with the remarkable property that it is independent of the generating function φ. Hence, as the field evolves through the sequence $\varphi_0 = \pi/2,\ \pi/4,\ 0,\ -(\pi/2)$, the magnetic energy at each point in the half space $z>0$ *remains constant.* The free energy of a magnetic field is the amount of magnetic energy in excess of the lowest minimum attributed to the potential field having the same normal field distribution at the boundary (Sturrock, 1967). Moreover, the potential field with this absolutely minimum energy is unique for a given boundary normal field distribution (Jackson, 1962). Let us look at the initial potential field $\mathbf{B}_{\text{pot}}$ with $\varphi_0 = \pi/2$. By the uniqueness theorem, we conclude there $\mathbf{B}_{\text{pot}}$ is at the lowest energy and there is no free energy in the system. For the other three configurations, $\varphi_0 = \pi/4,\ 0,\ -(\pi/2)$, we know the field is not potential in each case and therefore must be at a higher energy than that of its respective potential field. Thus, we conclude that free energy is available for these three configurations. In summary, as the field passes through the sequence $\varphi_0 = \pi/2,\ \pi/4,\ 0,\ -(\pi/2)$, the local energy density does not change but fractions of it become available to be liberated as free energy. In this sense, the field is evolving towards a flare producing stage.

To evaluate the actual amount of free energy available is not possible by analytic methods, as far as we can tell. The task involves solving for the potential field satisfying the same normal field distribution given in Equation (14). In terms of the Green's function, the potential field is $\mathbf{B} = \nabla\psi$ where (Levine, 1975)

$$\psi(x, y, z) = \int_{z=0} dx'\, dy' \frac{B_n(x', y')}{[(x-x')^2+(y-y')^2+z^2]^{1/2}}. \tag{21}$$

With the solution in explicit form, one goes on to compute the difference in energy between the force-free field given by Equations (11), (12), (13) and the potential field. In practice, a numerical method is needed for evaluating ψ (e.g., Schmidt, 1964; Levine, 1975; Sakurai, 1981b). In the paper to follow, we will compute the associated potential fields, both to evaluate the free energy and to compare the morphologies of both force-free and the associated potential field (Low and Chalmers, 1981). In calculating the free-energy, we do not need to know the values of

both the force-free and potential field everywhere. The photospheric values alone are sufficient to determine the free energy, as we show in the Appendix. This opens up the prospect that if we are able to improve the spatial resolution and the technology of vector magnetographs (Harvey, 1977; Stenflo, 1978; Hagyard *et al.*, 1981), we can evaluate magnetic free energy in the solar atmosphere without having to solve for non-linear force-free fields.

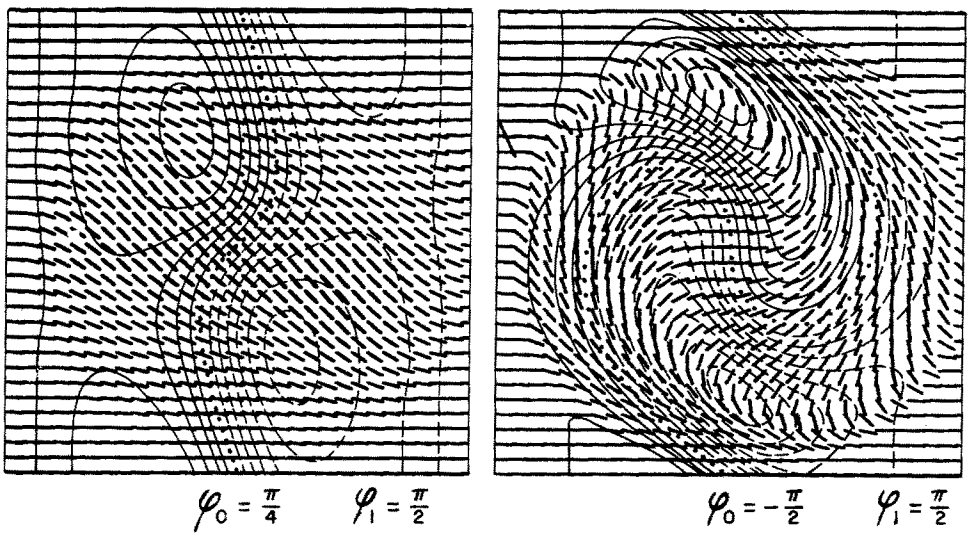

Fig. 4. Transverse field magnetograms for the force-free fields with $\varphi_1 = \pi/2$ and $\varphi_0 = \pi/4, -(\pi/2)$.

In Figure 4, we display the pattern of directions of the vector formed in the plane of the photosphere by the field components $B_x(x, y, 0)$ and $B_y(x, y, 0)$. Two cases are shown, $\varphi_0 = \pi/4$ and $\varphi_0 = -(\pi/2)$. These are theoretical examples of data that one would obtain from a vector magnetograph that measures the photospheric transverse field (Hagyard *et al.*, 1981). We have superposed our data against a backdrop of the contours of constant normal field $B_z(x, y, 0)$. Of particular interest are the regions around the points P^+ and P^-, marked in Figure 2 for visual clarity, where the transverse field aligns along the neutral line. Such features are absent in the $\varphi_0 = \pi/4$ data. Visual inspection of data for other values of φ_0 not presented here shows that as φ_0 increases, such an alignment forms progressively. Analyses of the Marshall Space Flight Center vector magnetograms show that the alignment of the transverse field with the neutral line is a strong indicator of a potential flare site (Smith *et al.*, 1981). We go on to consider the three dimensional field lines in this location and compare them with field lines elsewhere. We will find the former to be highly sheared low lying loops, a feature also known to be flare related (Vorpahl *et al.*, 1975; Petrasso *et al.*, 1975; Vorpahl, 1976; Su, 1980; Cheng, 1977). Our theoretical solution, thus, provides a theoretical association between these two independently observed flare features.

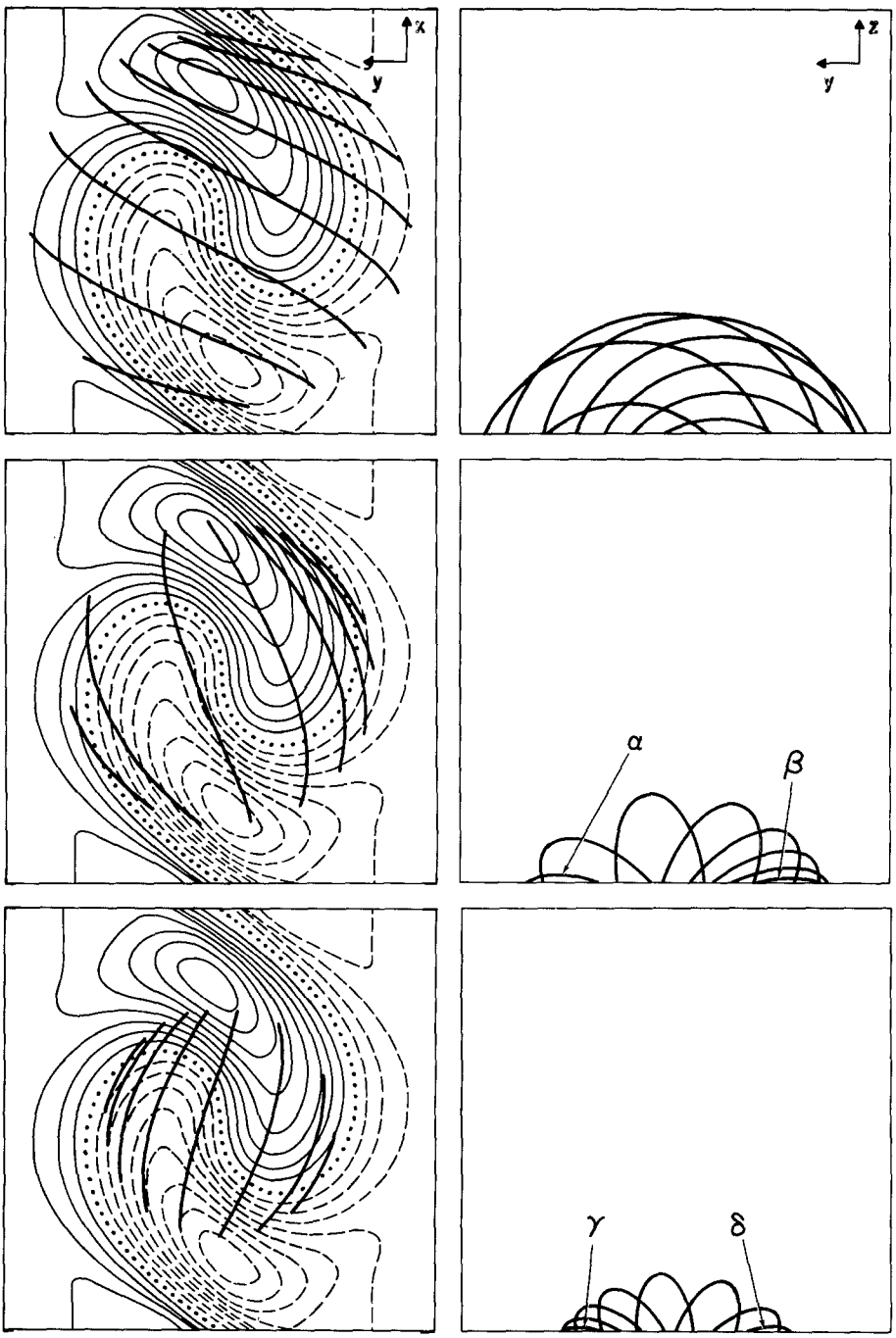

Fig. 5. Projected views of selected field lines of the force-free field with $\varphi_1 = \pi/2$ and $\varphi_0 = -(\pi/2)$.

The sub-figures in Figure 5 are plots of selected field lines of the $\varphi_0 = -(\pi/2)$ force-free field. The sub-figures on the left column shows sets of field lines with footpoints rooted on a circle of some selected radius, centered at $x = y = 0$ on the photosphere. These field lines are seen projected on the $x-y$ plane. In the background, we have the faint contours of constant $B_z(x, y, 0)$ for purpose of geometric reference. To indicate the height of these field lines, we plot in the corresponding sub-figures on the right column, the same set of field lines seen projected against the $y-z$ plane. With magnetograph data, it is the three dimensional view of the field lines above the photosphere that is not available because we cannot, in practice, extrapolate for the force-free field.

It is customary to assume that Hα fibrils are aligned along local magnetic fields (Zirin, 1972). If we were to select field lines from the three sets in Figure 5, identify them with Hα fibrils and view them projected on the x, y plane, the conspicuous feature of fibril-crossing' is produced (Zirin, 1970a). This flare related feature arises from the rotation of the spots, with field lines stretched and rotated beneath other field lines that suffer less changes because they are anchored in the quiet far regions. Notice that there are no field lines connecting the two regions of maximum $|B_z(x, y, 0)|$. Field lines from each of these regions lead to regions of weaker $|B_z(x, y, 0)|$. It is thus misleading to visualize, based on longitudinal magnetograms alone, the two regions of maximum $|B_z(x, y, 0)|$ to be the two ends of a flux rope.

We mark with Greek alphabets in Figure 5 the field lines located near $P_{\pm}$, characterized by the alignment of the photospheric transverse field with the neutral line. It is clear that these field lines, compared, to others are low lying, highly sheared to run almost parallel and above the neutral line. We suggest that such a setting is suited for the formation of a dark filament (Tandberg-Hanssen, 1974). To demonstrate filament structure requires taking gravity into account and this lies outside the scope of the force-free approximation. Moore and Zirin (unpublished), as reported by Kahler *et al.* (1980), found that a small low-lying dark filament can be found in association with almost every flare. If we view the magnetic field in terms of Equation (9) in polar coordinates, it is easy to see that progressive steepening $\varphi(r)$ leads to winding of the field line about the polar axis. On the plane $z = 0$, pairs of magnetic footpoints on either sides and near the neutral line approach each other as they are sheared along the neutral lines. Su (1980) has shown theoretically with a two-dimensional Cartesian model that this type of footpoint motion leads to low lying loops. It is also clear from the perspective of the polar coordinates that flux passes through the plane $z = 0$ by having field lines aligned along the neutral line and disappearing below $z = 0$. We suggest that this process leads to filament formation if the interaction between plasma gravity, and magnetic field were accounted for and the subsequent activation of the filament initiates the flare.

We return to Equation (10) to note that setting $\varphi(r)$ constant everywhere leads to $\alpha = 0$. Hence $\varphi = \pi/2$ is merely one of a class of potential fields. Let us look at other members of these potential fields. Figure 6 shows the two fields $\varphi = 0$ and

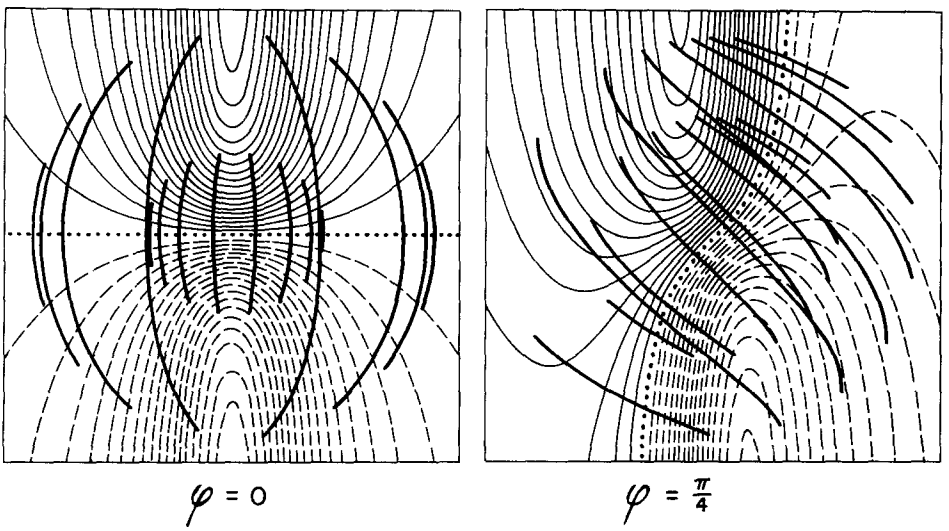

Fig. 6. The potential fields $\varphi = 0$ and $\varphi = \pi/4$.

$\varphi = \pi/4$. In the first, the contours of constant $B_z(x, y, 0)$ show a bipolar region symmetrically placed about a straight neutral line running on the y axis. The thick lines showing field lines projected on the xy plane exhibit no shear, or 'fibril-crossing'. In the second field, the bipolar field has a slant in its neutral line in the vicinity of the origin. The projected field lines also appear regular, without shear. This field is actually the linear superposition of the field $\varphi = \pi/2$, and $\varphi = 0$ as is evident from Equation (9) for a constant φ. The former is just the potential field $\mathbf{B}_{\text{pot}}$ given by Equation (3). Potential fields are linear.

We have considered the sequences of force-free fields generated by Equation (15) for different values of φ_0 and for $\varphi_1 = 0$ and $\pi/4$, respectively. In each case, we find the appearance of new spots which evolve into the polarity reversal configuration. The sequence beginning with $\varphi = 0$ is an interesting comparison with the previous sequence beginning with the $\varphi = \pi/2$ potential field that we analyzed in detail. The new sequence evolves with an increase in the total flux of a given sign. In other words, the appearance of spots and the reversal of polarities take place with the emergence of new flux through the photosphere. The integrated flux functions $f(\rho)$, which is the integrand appearing in Equation (17), for $\varphi_1 = 0$ and $\varphi_0 = 0$, $\pi/4$, $-(\pi/2)$, $-\pi$ are shown in Figure 3b. In Figure 7, we plot selected field lines in different projections for the case $\varphi_1 = 0, \varphi_0 = -\pi$ representing an advanced stage of spot growth and rotational motion. We find the polarity reversal is associated with developments of sheared low lying loops located where the photospheric transverse field aligns along the neutral line. In the perspective of the polar coordinates in Figure 1, it is in these localized regions where field lines emerge through the photosphere in the form of highly sheared loops.

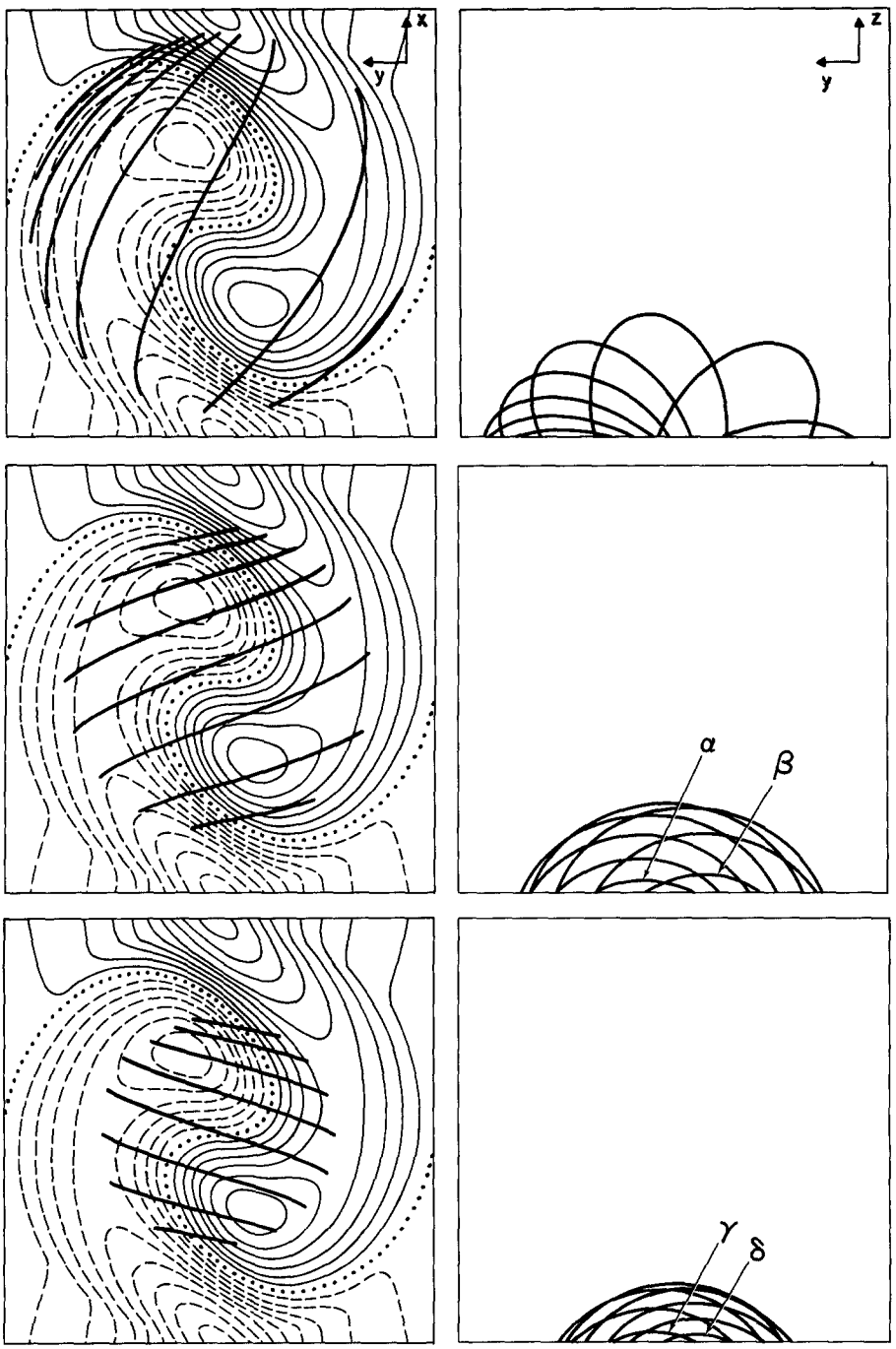

Fig. 7. The force-free field with $\varphi_1 = 0$ and $\varphi = -\pi$.

4. Discussion

In this paper, we have provided a theoretical relationship between different magnetic field features that have been identified separately by observation to indicate likely flare sites. In terms of sequences of exact force-free fields, we show by direct illustration how the global topology of the polarity reversal of a pair of spots implies local geometries of highly sheared, low lying loops in the vicinity where the photospheric transverse field aligns with the neutral line (Zirin, 1970a, b; Prata, 1972; Zirin and Tanaka, 1973; Vorpahl, 1976; Kahler *et al.*, 1975; Petrasso *et al.*, 1975; Vorpahl *et al.*, 1975; Zirin and Lazareff, 1975; Rust, 1976; Low, 1977a; Tanaka, 1976; Smith *et al.*, 1981). The formation of these sites is accompanied by the creation of magnetic free energy. The model also shows that as the field evolves, flux may emerge or disappear through the photosphere at these highly stressed locations. The association between flux emergence and flare eruption has been well documented (Rust, 1968; Vorpahl, 1973; Zirin and Tanaka, 1973; Rust *et al.*, 1975) and is the basis of some flare theories (Canfield *et al.*, 1974; Heyvaerts *et al.*, 1977). We suggest that flux may occasionally disappear below the photosphere at the neutral line, also leading to flare eruptions. What is important is whether the evolution, driven either by flux emergence or disappearance, brings about the availability of free energy to be released. As is well known, flares occur during both the build up and the decay phases of an active region. Rust (1976) draws the conclusion from various observations that except for the very large proton flares, the rate of change of flux involved in a flare do not differ from the normal growth or decay rates associated with sunspot fields (Rust, 1968, 1972, 1973; Livingston, 1974; Ribes, 1969).

We suggest the geometry of low-lying loops at a potential flare site is conducive to the formation of a dark filament. The destabilization of the filament, if it exists, may be an obvious agent initiating the flare, an idea made familiar by many observations of flares involving large and conspicuous filaments (Martin and Ramsey, 1972; Martin, 1973; Zirin and Tanaka, 1973; Roy and Tang, 1975; Rust *et al.*, 1975; Tanaka, 1976, etc). In this connection, the unpublished observations of Zirin and Moore is significant in that almost every flare is associated with a dark filament, often very small and not easy to detect.

In practice, we can only calculate for the potential field based on the longitudinal magnetograms. Even with better spatially resolved transverse magnetograms, the force-free field cannot be extrapolated. Without being able to compare the calculated potential field with the force-free field, no meaningful conclusion can be drawn on the amount of energy which is free for a flare release. The following converse situation emphasizes the point. The sequence of force-free fields shown in Figure 2 all have the *same* magnetic energy at each point in space. Without a comparison with the associated potential field, there is no way to know what fraction of the magnetic energy is free for each of the force-free field. This limitation of not being able to compare magnetic energies has contributed largely to the lack

of clear observational result on the relationship between magnetic energy and the flare. We will take up this matter in the next paper of this series where we will calculate the associated potential fields numerically and compare both potential and force-free fields in terms of their energy and field morphologies (Low and Chalmers, 1981). For the present, we wish to emphasize the practical importance of the formula in the Appendix for the total free energy, first derived by Molodensky (1974) for the purpose of theoretical stability analysis. It does not appear that the extrapolation of nonlinear force-free fields from magnetograms will be practical in the near future although work is in progress towards a numerical treatment (Sakurai, 1981a). The formula in the appendix allows us to calculate the free energy in terms of the photospheric vector field without the need to solve for the nonlinear force-free field everywhere. The free energy is a quantity of great physical significance in flare study. The prospect of being able to extract it directly from observational data should provide new incentives for improving the present technology of vector magnetograph as well as the theory of interpreting the magnetograph raw data.

Finally, the analytic force-free fields we analyzed are a special subset of the bigger class of fields generated by Equation (6). It will be interesting to go on to consider the models of this bigger class. A numerical study will probably be necessary.

Acknowledgements

Part of this work was done at NASA, Marshall Space Flight Center under a NRC-NASA Senior Research Associateship. The assistance of Ed Reichman with the computing facility of the Solar Maximum Mission group at Marshall is gratefully acknowledged. The author thanks Drs Grant Athay, Tom Holzer, and Art Hundhausen for reading and commenting on the paper and Ms Karen Lynch for typing the manuscript.

Appendix

Consider the vector identity (Chandrasekhar, 1961)

$$\mathbf{r}\cdot[(\nabla\times\mathbf{B})\times\mathbf{B}]=\tfrac{1}{2}B^2+\nabla\cdot[(\mathbf{B}\cdot\mathbf{r})\mathbf{B}-\tfrac{1}{2}B^2\mathbf{r}]\,. \tag{I.1}$$

Integrate over a volume V, making use of Gauss theorem to obtain

$$\int \mathbf{r}\cdot[(\nabla\times\mathbf{B})\times\mathbf{B}]\,\mathrm{d}V=\int_v \tfrac{1}{2}B^2\,\mathrm{d}V+\int_s [(\mathbf{B}\cdot\mathbf{r})B-\tfrac{1}{2}B^2\mathbf{r}]\cdot\mathrm{d}\mathbf{S}\,, \tag{I.2}$$

where S is the boundary surface of V. For a force-free field, the term on the left side vanishes giving

$$\int_v \frac{1}{8\pi}B^2\,\mathrm{d}V=\tfrac{1}{4}\pi\int_s \left[\tfrac{1}{2}B^2\mathbf{r}-(\mathbf{B}\cdot\mathbf{r})\mathbf{B}\right]\cdot\mathrm{d}\mathbf{S}\,. \tag{I.3}$$

Thus, the total magnetic energy of a force-free field is given by the field values at the boundary. This relationship was first derived by Molodensky (1974) in a theoretical discussion on stability. For application to the Sun, let $z = 0$ be the photosphere and consider a force-free field $\mathbf{B}^{ff}$ whose α vanishes in the far region $(x^2+y^2+z^2)^{1/2} \to \infty$. The field therefore deviates from the potential state only in a finite region centered around $x = y = z = 0$, such as those force-free fields treated in this paper. Now construct the potential field $\mathbf{B}^p$ having the same normal flux distribution at $z = 0$ as that of $\mathbf{B}^{ff}$ and having the same asymptotic values as $\mathbf{B}^{ff}$ in the far region $(x^2+y^2+z^2)^{1/2} \to \infty$. A unique solution exists and this potential field is the state of the absolutely lowest magnetic energy. The idea of the free magnetic energy derives from the consideration that when all the electric currents in the atmosphere $z > 0$ are dissipated in a flare, what is left in $z > 0$ would be the potential field $\mathbf{B}^p$ due to electric currents below $z = 0$, which is assumed to be unchanged in the process. The free magnetic energy is thus

$$\Delta E = \frac{1}{8\pi} \int_{z>0} (\mathbf{B}^{ff} \cdot \mathbf{B}^{ff} - \mathbf{B}^p \cdot \mathbf{B}^p)\, \mathrm{d}V \tag{I.4}$$

Since $\mathbf{B}^{ff}$ and $\mathbf{B}^p$ are both force-free, a direct application of (I.3) gives

$$\Delta E = \frac{1}{4\pi} \int_{z=0} \mathrm{d}x\, \mathrm{d}y\, [x(B_s^{ff} - B_x^p) + y(B_y^{ff} - B_y^p)] B_z^{ff}, \tag{I.5}$$

the other surface integrals having dropped out since $\mathbf{B}^{ff}$ and $\mathbf{B}^p$ are equal on those surfaces. In practice, the three components of $\mathbf{B}^{ff}$ at $z = 0$ are to be provided by a vector magnetograph. Based on the $B_z^{ff}(x, y, 0)$ given, the potential field $\mathbf{B}^p$ is constructed by, say, the Schmidt program (Schmidt, 1964). From the potential solution, we obtain the x and y components of $\mathbf{B}^p$ at $z = 0$. We then have sufficient information to evaluate the free energy ΔE.

The formula (I.3) can be extended from the virial theorem to the case of a field which is not force-free but in static equilibrium with plasma pressure and gravity (Low, 1980b).

References

Barnes, C. W. and Sturrock, P. A.: 1972, *Astrophys. J.* **174**, 659.

Birn, J., Goldstein, H., and Schindler, K.: 1978, *Solar Phys.* **57**, 81.

Beckers, J. M.: 1971, in R. Howard (ed.), 'Solar Magnetic Fields', *IAU Symp.* **43**, 3.

Canfield, R. C., Priest, E. R., and Rust, D. M.: 1974, in *Flare Related Magnetic Field Dynamics*, NCAR, p. 361.

Chandrasekhar, S.: 1961, *Hydrodynamic and Hydromagnetic Stability*, Oxford Univ. Press.

Chandrasekhar, S. and Kendall, P. C.: 1957, *Astrophys. J.* **126**, 457.

Cheng, C. C.: 1977, *Solar Phys.* **55**, 413.

Cohen, R. H., Coppi, B., and Treves, A.: 1973, *Astrophys. J.* **179**, 269.

Gold, T.: 1964, in W. N. Hess (ed.), *AAS-NASA Symp. Physics of Solar Flares*, NASA, p. 389.

Hagyard, M. J., Cumings, N. P., and West, E. A.: 1981, *Rev. Scientific Instruments*, (submitted).
Harvey, J. W.: 1977, *Highlights of Astronomy* **4**, 223.
Heyvaerts, J., Priest, E. R., and Rust, D. M.: 1977, *Astrophys. J.* **216**, 123.
Jackson, J. D.: 1962, *Classical Electrodynamics*, Wiley, New York.
Jockers, K.: 1978, *Solar Phys.* **56**, 37.
Kahler, S. W., Krieger, A. S., and Vaiana, C. S.: 1975, *Astrophys. J. Letters* **199**, L57.
Kahler, S. W., Spicer, D., Uchida, Y., and Zirin, H.: 1980, in P. A. Sturrock (ed.), *Solar Flares*, Colorado Associated Univ. Press, p. 83.
Levine, R. H.: 1975, *Solar Phys.* **44**, 365.
Livingston, W. C.: 1974, in *Flare Related Magnetic Field Dynamics*, NCAR, p. 269.
Low, B. C.: 1977a, *Astrophys. J.* **212**, 234.
Low, B. C.: 1977b, *Astrophys. J.* **217**, 988.
Low, B. C.: 1980a, *Astrophys. J.* **239**, 377.
Low, B. C.: 1980b, MSFC/NASA Preprint.
Low, B. C.: 1982, *Rev. Geophys. Space Phys.*, (in press).
Low, B. C. and Chalmers, J.: 1981, in preparation.
Lüst, R. and Schlüter, A.: 1954, *Z. Astrophys.* **34**, 263, 365.
Martin, S. F.: 1973, *Solar Phys.* **31**, 3.
Martin, S. F. and Ramsey, H. E.: 1972, in P. McIntosh and M. Dryer (eds.), *Solar Activity Observations and Predictions*, MIT Press, p. 371.
Milsom, F. and Wright, G. A. E.: 1976, *Monthly Notices Roy. Astron. Soc.* **174**, 307.
Molodensky, M. M.: 1974, *Solar Phys.* **39**, 393.
Morikawa, G. K.: 1969, *Phys. Fluid* **12**, 1648.
Nakagawa, Y. and Raadu, M. A.: 1972, *Solar Phys.* **25**, 127.
Petrasso, R. D., Kahler, S. W., Krieger, A. S., Silk, J. K., and Vaiana, G. S.: 1975, *Astrophys. J. Letters* **199**, L127.
Prata, S. W.: 1972, *Solar Phys.* **25**, 36.
Priest, E. R. and Milne, A. M.: 1980, *Solar Phys.* **65**, 315.
Ribes, E.: 1969, *Astron. Astrophys.* **2**, 316.
Roy, T.-R. and Tang, F.: 1975, *Solar Phys.* **42**, 425.
Rust, D. M.: 1968, in K. O. Kiepenheuer (ed.), 'Structure and Development of Solar Active Regions', *IAU Symp.* **35**, 77.
Rust, D. M.: 1972, *Solar Phys.* **25**, 141.
Rust, D. M.: 1973, *Solar Phys.* **33**, 205.
Rust, D. M.: 1976, *Solar Phys.* **47**, 21.
Rust, D. M., Nakagawa, Y., and Neupert, W. M.: 1975, *Solar Phys.* **41**, 397.
Sakurai, T.: 1979, *Publ. Astron. Soc. Japan*, **31**, 209.
Sakurai, T.: 1981a, *Solar Phys.* **69**, 343.
Sakurai, T.: 1981b, preprint.
Schmidt, H.: 1964, in W. N. Hess (ed.), *AAS-NASA Symp. Physics of Solar Flares*, NASA, p. 107.
Schmidt, H.: 1968, in K. O. Kiepenheuer (ed.), 'Structure and Development of Solar Active Regions', *IAU Symp.* **35**, 95.
Smith, Jr., J. B., Hagyard, M. J., and Krall, K.: 1981, preprint.
Stenflo, J. O.: 1978, *Rep. Prog. Phys.* **41**, 865.
Sturrock, P. A.: 1967, in P. A. Sturrock (ed.), *Plasma Astrophysics*, Academic Press, p. 168.
Sturrock, P. A. (ed.): 1980, *Solar Flares*, Colorado Assoc. Univ. Press.
Sturrock, P. A. and Woodbury, E. T.: 1967, in P. A. Sturrock (ed.), *Plasma Astrophysics*, Academic Press, p. 155.
Su, Q.-R.: 1980, *Acta Astron. Sinica* **21**, 152.
Švestka, Z.: 1976, *Solar Flares*, D. Reidel Publ. Co., Dordrecht, Holland.
Tanaka, K.: 1976, *Solar Phys.* **47**, 247.
Tandberg-Hanssen, E.: 1974, *Solar Prominences*, D. Reidel Publ. Co., Dordrecht, Holland.
Vorpahl, J. A.: 1973, *Solar Phys.* **28**, 115.
Vorpahl, J. A.: 1976, *Astrophys. J.* **205**, 868.
Vorpahl, J. A., Gibson, E. G., Landecker, P. B., McKenzie, D. L., and Underwood, J. H.: 1975, *Solar Phys.* **45**, 199.

Zirin, H.: 1970a, *Solar Phys.* **14**, 428.
Zirin, H.: 1970b, *Solar Phys.* **14**, 342.
Zirin, H.: 1972, *Solar Phys.* **22**, 34.
Zirin, H.: 1974, *Vistas Astron.* **16**, 1.
Zirin, H. and Lazareff, B.: 1975, *Solar Phys.* **41**, 425.
Zirin, H. and Tanaka, K.: 1973, *Solar Phys.* **32**, 173.